SANDIA REPORT
SAND2003-1352
Unlimited Release
Printed May/2003

A Theory for RF and Microwave Scalar Reflectometers

Robert D. Moyer

Prepared by
Sandia National Laboratories
Albuquerque, New Mexico 87185 and Livermore, California 94550

Sandia is a multiprogram laboratory operated by Sandia Corporation,
a Lockheed Martin Company, for the United States Department of Energy's
National Nuclear Security Administration under Contract DE-AC04-94AL85000.

Sandia National Laboratories

Issued by Sandia National Laboratories, operated for the United States Department of Energy by Sandia Corporation.

Available to DOE and DOE contractors from
U.S. Department of Energy
Office of Scientific and Technical Information
P.O. Box 62
Oak Ridge, TN 37831

Telephone: (865)576-8401
Facsimile: (865)576-5728
E-Mail: reports@adonis.osti.gov
Online ordering: http://www.doe.gov/bridge

Available to the public from
U.S. Department of Commerce
National Technical Information Service
5285 Port Royal Rd
Springfield, VA 22161

Telephone: (800)553-6847
Facsimile: (703)605-6900
E-Mail: orders@ntis.fedworld.gov
Online order: http://www.ntis.gov/help/ordermethods.asp?loc=7-4-0#online

SAND2003-1352
Unlimited Release
Printed April 2003

A Theory for RF and Microwave Scalar Reflectometers

Robert D. Moyer
Primary Electrical Standards Department
Sandia National Laboratories
P.O. Box 5800
Albuquerque, NM 87185-0665

Abstract

A careful analysis of rf and microwave scalar reflectometers is conducted to (1) reveal the advantages of 4-port over 3-port reflectometers, (2) show the advantage – and remaining weaknesses – of a reflectometer initialized by the open/short method and (3) present expressions for the worst-case errors in scalar reflectometer measurements.

Introduction

RF and microwave reflectometers are often used in conjunction with scalar receivers to make moderate accuracy reflection coefficient measurements. This report discusses the theory involved in such measurements in the following five different sections:

I. Representation of reflectometers and notation.
II. A good way to initialize a scalar 4-port reflectometer.
III. Irrelevance of detector reflection coefficients.
IV. Advantages of a 4-port reflectometer over a 3-port reflectometer.
V. Worst-Case Errors of a well-initialized scalar 4-port reflectometer.

I. Representation of reflectometers and notation.

Figures 1a and 1b show schematic representations of 4-port reflectometers based on a directional coupler and a power splitter–directional bridge combination, respectively. For analysis purposes, Figure 1c shows the signal flow diagram representation of a 4-port reflectometer. A signal source - whose internal source reflection coefficient is g - drives port 1 of the reflectometer. The initialization and unknown devices are connected to port 2 - the test port. The true reflection coefficient of any device connected to test port 2 is denoted as z. The signal measured at port 3 is primarily proportional to the signal emergent from test port 2 of the reflectometer (i.e. incident on the device connected to port 2) while the signal measured at port 4 is primarily proportional to the signal reflected from the device connected to test port 2. Thus, the ratio of the latter signal to the former signal is approximately proportional to the reflection coefficient of the device connected to port 2. The ratio of the traveling wave voltage emergent from port 4, b_4, to the traveling wave voltage emergent from the generator, b_G, may be found from the signal flow graph as

$$\frac{b_4}{b_G} = \frac{S_{41}(1 - zS_{22}) + S_{21}zS_{42}}{1 - gS_{11} - zS_{22} + gS_{11}zS_{22} - gS_{21}zS_{12}} = \frac{z\left(\frac{S_{21}S_{42} - S_{22}S_{41}}{1 - gS_{11}}\right) + \frac{S_{41}}{1 - gS_{11}}}{z\left(\frac{gS_{11}S_{22} - gS_{21}S_{12} - S_{22}}{1 - gS_{11}}\right) + 1} = \frac{hz + e}{fz + 1} \quad (1)$$

where:

- h, e and f are functions of g and the S-parameters of the reflectometer as suggested in equation (1);
- ρ_3 and ρ_4 (in Figure 1c) are the reflection coefficients of the detectors on ports 3 and 4, respectively;
- ρ_3 and ρ_4 were set to 0 during the derivation of equation (1) in anticipation of the result of section III. (There it is shown that the values of ρ_3 and ρ_4 are arbitrary when the reflectometer is initialized by the preferred technique described in section II.) Equations (1) through (4) would be much more cumbersome if $\rho_3 \neq 0$ and $\rho_4 \neq 0$.

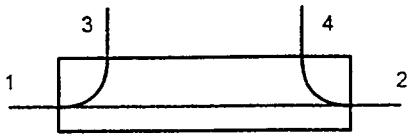

Figure 1a. Directional Coupler

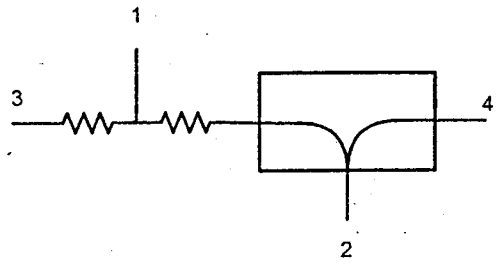

Figure 1b. Splitter - Directional Bridge

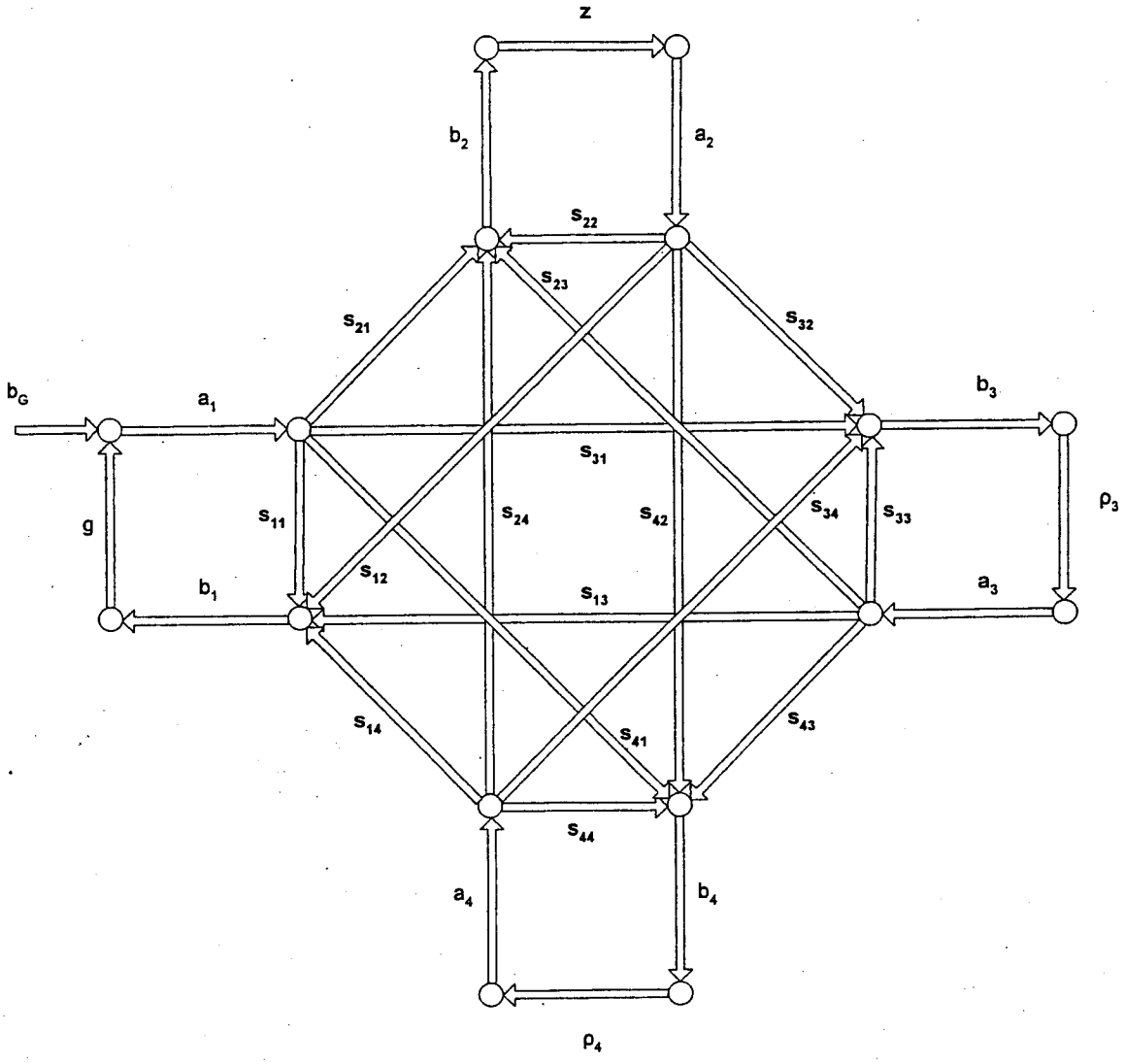

Figure 1c. 4-Port Signal Flow Diagram

Similarly,

$$\frac{b_3}{b_G} = \frac{z\left(\frac{S_{21}S_{32} - S_{22}S_{31}}{1 - gS_{11}}\right) + \frac{S_{31}}{1 - gS_{11}}}{z\left(\frac{gS_{11}S_{22} - gS_{21}S_{12} - S_{22}}{1 - gS_{11}}\right) + 1} \quad . \tag{2}$$

Taking the ratio of the preceding two equations gives the measured ratio, w_m, of the emergent traveling wave voltage from port 4 to that at port 3 as

$$w_m = \frac{b_4}{b_3} = \frac{z(S_{21}S_{42} - S_{22}S_{41}) + S_{41}}{z(S_{21}S_{32} - S_{22}S_{31}) + S_{31}} \tag{3}$$

or

$$w_m = \frac{b_4}{b_3} = \frac{z\left(S_{21}S_{42} - S_{22}S_{41}\right)/S_{31} + S_{41}/S_{31}}{-z\left(S_{22} - \frac{S_{21}S_{32}}{S_{31}}\right) + 1} = \frac{qz + r}{sz + 1} \tag{4}$$

where q, r and s are complex functions of the S-parameters of the reflectometer as indicated in equation (4).

For 3-port reflectometers, one uses equation (1) for the measured ratio because port 3 is not present; for 4-port reflectometers, one uses equation (4).

II. A good way to initialize scalar reflectometers.

If a vector receiver is available to measure the complex ratios and the complex S-parameters of the reflectometer are known, then very accurate reflection coefficient measurements can be made. It is, however, much less expensive to use scalar sensors, which respond only to amplitudes, on a reflectometer; unfortunately, accuracy decreases when scalar detectors are used. This section discusses a way to mitigate the loss of accuracy through use of a well-known initialization procedure.

Equations (1) and (4) show that both b_4/b_G (measured on a 3-port reflectometer) and b_4/b_3 (measured on a 4-port reflectometer) are given by linear fractional expressions. Because of this, the development in this section II is applicable to both 3- and 4-port reflectometers. For convenience, the development will be carried out using the notation for the 4-port reflectometer.

When making scalar reflectometer measurements, one must take the magnitude of equation (4) to obtain

$$|w_m| = \frac{|b_4|}{|b_3|} = \frac{|qz + r|}{|sz + 1|}. \tag{5}$$

Of course, it is desirable to obtain an estimator from the scalar reflectometer that very closely approximates $|z|$. Clearly, $|w_m|$ is not that estimator since the parameter q may differ significantly from unity. The desired estimator can be found by "initializing" the 4-port reflectometer.

First, a poor way to initialize the reflectometer is described in the following 3 steps:

Step 1: Measure an open circuit, i.e. $z = e^{-j\phi}$, at test port 2 which gives

$$|w_o| = \frac{|qe^{-j\phi} + r|}{|se^{-j\phi} + 1|}. \tag{6}$$

Step 2: Divide equation (5) – which results from measuring the unknown device - by equation (6) to obtain

$$\frac{|w_m|}{|w_o|} = \frac{|qz + r|}{|sz + 1|}\frac{|se^{-j\phi} + 1|}{|qe^{-j\phi} + r|} = \frac{\left|zq\frac{|se^{-j\phi} + 1|}{|qe^{-j\phi} + r|} + r\frac{|se^{-j\phi} + 1|}{|qe^{-j\phi} + r|}\right|}{|sz + 1|} \tag{7}$$

or

$$\frac{|w_m|}{|w_o|} = \frac{|zq' + r'|}{|sz + 1|}. \tag{8}$$

Step 3: Equation (8) shows that the estimator $|w_m/w_o|$ equals $|z|$ IF $r' = s = 0$ and $|q'| = 1$. Unfortunately, r' and s are often large enough to cause significant errors themselves and they drive $|q'|$ [equation (8)] away from unity because q' has **first** order dependence on r and s as seen in equation (7).

A preferred, well-known, procedure for initialization is given in step 4 through step 6 which follow:

Step 4: Measure the unknown and open circuit to get equations (5) and (6) as shown above.

Step 5: Measure an offset short circuit, i.e. $z = e^{-j(\pi+\phi)}$, which is 180 degrees out of phase with the open circuit, to get

$$|w_s| = \frac{|qe^{-j(\pi+\phi)} + r|}{|se^{-j(\pi+\phi)} + 1|} = \frac{|-qe^{-j\phi} + r|}{|-se^{-j\phi} + 1|}. \tag{9}$$

Step 6: Divide equation (5) by the square root of the product of equations (6) and (9) to obtain

$$\frac{|w_m|}{\sqrt{|w_s||w_o|}} = \frac{|qz + r|}{|sz + 1|}\sqrt{\frac{|se^{-j\phi} + 1|}{|qe^{-j\phi} + r|}\frac{|-se^{-j\phi} + 1|}{|-qe^{-j\phi} + r|}}$$

or

$$\frac{|w_m|}{\sqrt{|w_s||w_o|}} = \frac{|qz + r|}{|sz + 1|}\sqrt{\frac{|-s^2e^{-j2\phi} + 1|}{|-q^2e^{-j2\phi} + r^2|}}$$

or

$$\frac{|w_m|}{\sqrt{|w_s||w_o|}} = \frac{\left|q\sqrt{\frac{|-s^2e^{-j2\phi} + 1|}{|-q^2e^{-j2\phi} + r^2|}}z + r\sqrt{\frac{|-s^2e^{-j2\phi} + 1|}{|-q^2e^{-j2\phi} + r^2|}}\right|}{|sz + 1|} \tag{10}$$

or

$$\frac{|w_m|}{\sqrt{|w_s||w_o|}} = \frac{|q''z + r''|}{|sz + 1|}. \tag{11}$$

where q" is the coefficient of z in the numerator of (10) and r" is the final term in that numerator. From equation (4), it follows that

$$\frac{r}{q} = \frac{S_{41}}{S_{21}S_{42} - S_{22}S_{41}} \approx \frac{S_{41}}{S_{21}S_{42}} \tag{12}$$

where the approximation holds because $|S_{22}S_{41}| << |S_{21}S_{42}|$ for both circuits shown in Figure 1. Furthermore, $|r/q| \approx |d| << 1$ since the coupler or directional bridge will have high directivity, i.e. very small $|d| = |S_{41}/S_{42}|$, if it is used in a reflectometer application. Also, as previously mentioned, $|s|^2 << 1$ so the (twice- occurring) radical in the numerator of equation (10) reduces to approximately $|1/q|$.

Equations (10) and (11) therefore show that $\frac{|w_m|}{\sqrt{|w_s||w_o|}}$ is a better estimator because q" has only **second** order dependence on the small, but inevitably present, r and s parameters! |q"| will therefore more closely approximate unity than does |q'| as defined by equations (7) and (8). Steps 4 through 6 therefore define a preferred technique for initializing a scalar reflectometer.

While use of the open-short initialization technique gives a very good value of q", the same cannot, unfortunately, be said for r" and s. Equations (7), (8), (10) and (11) show that the value of s in the denominator is **not** affected at all by the preferred initialization process. Secondly, in equation (11), $|r"| \approx |r/q| \approx |d|$, so the effective directivity, |r"|, remains approximately equal to the device directivity |d|. Consequently, measurements of unknowns will still be in error due to both the directivity of the directional device and multiple reflections between the unknown and the effective source match of the reflectometer.

III. Irrelevance of detector reflection coefficients.

Equations (1) through (4) characterize the traveling wave voltage amplitudes while most detectors respond to power. Furthermore, detectors always reflect a small portion of any signal incident upon them. However, the reflection coefficients (ρ_3 and ρ_4 in Figure 1c) of the detectors do not influence the results from a scalar reflectometer that is initialized by the preferred technique described in the preceeding section. Again, this is true for both 3- and 4-port reflectometers as shown in the following paragraphs.

Of course in practice, power, rather than b_{ix}, (i = 3 or 4; x = m, s or o) is measured at each sidearm port of a scalar reflectometer. The relationship

$$\left|\frac{b_{4x}}{b_{3x}}\right| = \sqrt{\frac{P_{4x}Z_0\left(1-\rho_3^2\right)}{\left(1-\rho_4^2\right)P_{3x}Z_0}} = \sqrt{\frac{P_{4x}\left(1-\rho_3^2\right)}{\left(1-\rho_4^2\right)P_{3x}}} \tag{13}$$

shows a familiar relationship between powers and traveling voltage waves where

P_{ix} is the power absorbed by detector i when voltage wave b_{ix} is incident on it;

Z_0 is the (real) characteristic impedance of the system;

ρ_i is the magnitude of the reflection coefficient of detector i.

Using this relationship and refering to equations (4) and (11), the preferred estimator for a 4-port scalar reflectometer is given by

$$\frac{\left|\frac{b_{4m}}{b_{3m}}\right|}{\sqrt{\left|\frac{b_{4s}}{b_{3s}}\right|\left|\frac{b_{4o}}{b_{3o}}\right|}} = \frac{\sqrt{\frac{P_{4m}\left(1-\rho_3^2\right)}{\left(1-\rho_4^2\right)P_{3m}}}}{\sqrt{\sqrt{\frac{P_{4s}\left(1-\rho_3^2\right)}{\left(1-\rho_4^2\right)P_{3s}}}\sqrt{\frac{P_{4o}\left(1-\rho_3^2\right)}{\left(1-\rho_4^2\right)P_{3o}}}}} = \frac{\sqrt{\frac{P_{4m}}{P_{3m}}}}{\sqrt{\sqrt{\frac{P_{4s}}{P_{3s}}}\sqrt{\frac{P_{4o}}{P_{3o}}}}}. \tag{14}$$

This shows that the preferred estimator is independent of both detector reflection coefficients.

IV. Advantages of a 4-port reflectometer over a 3-port reflectometer.

It is important to notice that parameters q, r and s in equation (4) are entirely independent of g - the reflection coefficient of the source which drives the 4-port reflectometer. (Note that $-s = \Gamma_{ge}$, the effective generator reflection coefficient[2] of the 4-port reflectometer. In general, $|\Gamma_{ge}|$ will be significantly smaller than |g|.) It therefore follows that the preferred estimator - see equation (11) - for a 4-port scalar reflectometer is also independent of g. On the other hand, if a 3-port reflectometer is used, one must work with equation (1) because port 3 does not exist. In this case, the parameter f in equation (1) has three terms which depend on g ; the $gS_{21}S_{12}$ term, in particular, can be large enough to cause significant errors in the measured reflection coefficient. Furthermore, it was pointed out in the last paragraph of section II that the parameter s (for a 4-port reflectometer) is not diminished by use of the preferred initialization procedure; it is easily shown that the same is true of the parameter f for the 3-port reflectometer. The parameter f – and therefore the error in measurements from a 3-port reflectometer – changes whenever g (the source reflection coefficient of the generator driving the 3-port reflectometer) changes.

Based on these considerations, two significant advantages of the 4-port reflectometer are:

1. The performance of the 4-port reflectometer is independent of g, the reflection coefficient of the source which drives it, while a 3-port reflectometer's performance does depend on the reflection coefficient of its driving source.

2. If b_3 and b_4 are measured simultaneously, the 4-port reflectometer is immune to variations in level from the source. On the other hand, the 3-port reflectometer provides no mechanism for eliminating the effects of source level variations between measurements.

V. Worst-Case Errors on measurements from a well-initialized scalar 4-port reflectometer

Equation (11), as a real equation, specifies the preferred estimator from a **scalar** reflectometer; the magnitude bars are required because the scalar detectors cannot sense vector information. However, the error mechanisms in the scalar reflectometer are vector in nature. In order to characterize the errors in the scalar estimator, it is necessary to analyze the vector relationships obtained by removing the magnitude restraints from equation (11). Thus:

$$\frac{w_m}{\sqrt{w_s w_o}} = \frac{q''z + r''}{sz + 1} = w \tag{15}$$

Equation (15) shows that w, the preferred estimator for a 4-port scalar reflectometer, is a complex bilinear transformation of z, the true reflection coefficient of the device being measured.

Inverting equation (15) gives

$$z = \frac{w - r''}{-sw + q''} = \frac{a''w + b''}{cw + 1}. \tag{16}$$

Therefore, if the locus of w is a circle at the origin of the complex plane, the locus of z will be another circle of radius R_1 whose center lies at the tip of a vector C_1. According to equations (2.153) and (2.154) of Reference (1), R_1 and C_1 are given by

$$R_1 = \frac{|a''-b''c||w|}{1-|cw|^2} \tag{2.153}$$

and

$$C_1 = \frac{b''-a''c^*|w|^2}{1-|cw|^2}, \text{ respectively.} \tag{2.154}$$

Knowing that $|a''| \sim 1$, $|b''| < 1$ and $|c| < 1$ for a well-initialized 4-port scalar reflectometer, equation (2.153) shows that R_1 will be approximately equal to $|w|$ while equation (2.154) shows that $|C_1|$ will very likely exceed R_1 for small values of $|w|$. Figure 2 depicts a possible relationship between the locus of w - which is centered at the origin - and the locus of z – which is centered at the tip of C_1.

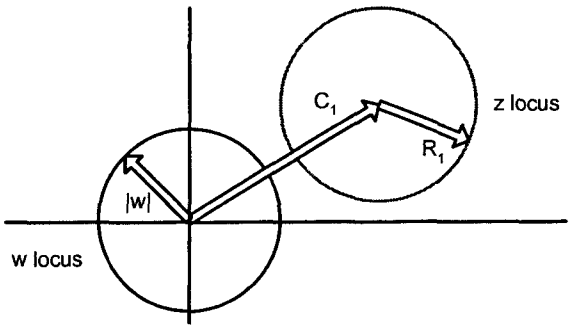

Figure 2 A possible relationship between w and z loci.

The worst-case error at a given frequency f, WCE_f, in a scalar reflectometer measurement, $|w|$, is the largest difference between $|w|$ and $|z|$. It is given by the expressions (see Appendix)

$WCE_f = |C_1| + R_1 - |w|$ if $R_1 > |w|$ or $|C_1| > |w|$. (17a)

If $|w| > R_1 > |C_1|$ then $WCE_f = |C_1| - R_1 + |w|$. (17b)

If $|w| > |C_1| > R_1$ then $WCE_f = |C_1| - R_1 - |w|$. (17c)

Some important remarks about application of equations (17) are in order. If one uses the complex values (at a given frequency f) of a", b" and c to compute the values of R_1 and $|C_1|$, then using the appropriate equation of (17) gives WCE_f, the worst-case error **with respect to all possible phases of w at frequency f.** However, WCE_f is **not** worst-case with respect to all possible phases of a", b" and c at frequency f.

The following development leads to generalized expressions [see equations (22) below] for the worst-case errors with respect to all possible phases of w as well as those of a", b" and c.

From equations (2.153) and (2.154), one can compute

$$|C_1|^2 - R_1^2 = \frac{|b"|^2 - |a"|^2|w|^2}{1-|c|^2|w|^2}$$

or

$$(|C_1|+R_1)(|C_1|-R_1) = \left(\frac{|b"| + |a"||w|}{1-|c||w|}\right)\left(\frac{|b"| - |a"||w|}{1+|c||w|}\right) \qquad (18)$$

Combining equations (17a), (17b) and (17c) with (18) gives

$$WCE = \left(\frac{|b"| + |a"||w|}{1-|c||w|}\right) - |w| \quad \text{if } R_1 > |w| \text{ or } |C_1| > |w| \qquad (19a)$$

where WCE is the worst-case error with respect to all possible phases of w, a", b" and c.

$$WCE = \left(\frac{|b"| - |a"||w|}{1+|c||w|}\right) + |w| \quad \text{if } |w| > R_1 > |C_1| \qquad (19b)$$

and finally,

$$WCE = \left(\frac{|b"| - |a"||w|}{1+|c||w|}\right) - |w| \quad \text{if } |w| > |C_1| > R_1. \qquad (19c)$$

By use of a Taylor's series, assuming that $|c||w| \ll 1$,

$$\frac{1}{1\pm|c||w|} = 1\mp|c||w| + |c|^2|w|^2 \mp \ldots . \qquad (20)$$

Substituting (20) into (19a) gives (21) i.e.

$$WCE = |b"| + |w|(|a"| - 1 + |cb"|) + |w|^2(|ca"| + |c|^2|b"|) + |w|^3(|c|^2|a"| + |c|^3|b"|) + \ldots$$

Recalling that $|c| \cong |b"| \ll |a"| \cong 1$ in a well-initialized 4-port reflectometer, it is apparent that all terms in $|w|^n$ - where n>2 - in equation (21) can be dropped giving – subject to the conditions $R_1 > |w|$ or $|C_1| > |w|$ -

$$WCE \cong |b"| - |w|(1 - |a"| - |cb"|) + |w|^2(|ca"| + |c|^2|b"|). \qquad (22a)$$

Analogously, equation (19b) may be re-written as, subject to the conditions $|w| > R_1 > |C_1|$,

$$WCE \cong |b"| + |w|(1 - |a"| - |cb"|) + |w|^2(|ca"| + |c|^2|b"|). \qquad (22b)$$

Finally, equation (19c) may be rewritten as – subject to the conditions $|w| > |C_1| > R_1$ -

$$WCE \cong |b''| - |w|(1+|a''|+|cb''|)+|w|^2\,(|ca''|+|c|^2|b''|)\,. \qquad (22c)$$

A significant conclusion to be drawn from equations (22a), (22b) and (22c) is that they may be generalized to the form

$$WCE \cong \alpha + \beta|w| + \gamma|w|^2\,. \qquad (23)$$

This shows that the worst-case error – **with respect to all possible phases of w, a, b and c** - from a well-initialized 4-port scalar reflectometer can be adequately expressed as a quadratic function of |w|. The values of the real parameters α, β and γ characterize a particular scalar reflectometer **over a frequency band** where the phases of a, b and c may assume any values. Note that 1) the parameters α and γ are always positive and 2) the worst-case error includes a (usually small) term proportional to |w| - even for a well-initialized scalar reflectometer.

It is important to recognize that, **at a particular frequency**, WCE_f may either **increase** or **decrease** as |w| increases. This is demonstrated in the following table where values of WCE_f are computed for a scalar reflectometer having typical values a" = 1, b" = 0.01 and |c| = 0.1. In the first two cases considered, the phase of c is 0 degrees; in the final two cases, the phase of c is 180 degrees. Cases 1 and 3 show the situation when the measured reflection coefficient is |w| = 0.1 while cases 2 and 4 apply when |w| = 0.3. The fourth and fifth columns give calculated (see equations 2.153 and 2.154) values for radius R_1 and magnitude of vector C_1, respectively, which result from the specified values of a", b" c and |w|. The sixth column identifies the appropriate – as determined by the relative values of |w|, R_1 and $|C_1|$ - equation for computing WCE_f. Finally, the computed value of WCE_f appears in the seventh column.

Case	c	|w|	R_1	$\|C_1\|$	Equation	WCE_f
1	0.1	0.1	0.09991	0.009	(17b)	0.009
2	0.1	0.3	0.29997	0.001	(17b)	0.001
3	-0.1	0.1	0.10011	0.011	(17a)	0.011
4	-0.1	0.3	0.30057	0.019	(17a)	0.020

Table 1. Dependence of WCE_f on |w| and phase of c

Notice that WCE_f decreases as |w| increases when the phase of c is 0 in cases 1 and 2. On the other hand, WCE_f increases with increasing |w| when the phase of c is 180 degrees.

The expressions for worst-case error, WCE_f, given in equations (17) followed quite naturally from the physical operation of a 4-port scalar reflectometer. To conform with current popular practice, one could try to re-cast these expressions into "standard uncertainties" or "expanded uncertainties" as recommended by the U.S. Guide to the Expression of Uncertainty in Measurement[3]. It appears, however, that this would not be appropriate. Paragraph 3.2.4 of the Guide states

> "It is assumed that the result of a measurement has been corrected for all recognized significant systematic effects and that every effort has been made to identify such effects."

There are three sources of systematic effects in the expression for w from a scalar reflectometer, namely the q", r" and s parameters in equation (15). These quantities are recognized, significant and produce systematic effects that depend on the value of the device measured. Equations (2.153) and (2.154) lead to Figure 2 which graphically shows the systematic effects of the three

error sources. While it is possible to correct for these systematic effects in **vector** network analyzer systems, it is not possible in **scalar** systems.

The Guide does offer an example (in section F.2.4.5) of a way to incorporate "a single mean correction" into the combined variance to accommodate situations where it is impossible or undesirable to eliminate known systematic effects. It appears, however, that such a procedure would produce an uncertainty statement of no added value. Rather, it would produce one that weakens the relationship between the uncertainty statement and the physical processes – as shown in Figure 2 - in the reflectometer which cause the errors.

Summary

It has been shown that the performance of a 4-port scalar reflectometer is entirely independent of the level instability (if the detector outputs 3 and 4 are measured simultaneously) and source reflection coefficient of its driving source. A 3-port reflectometer is vulnerable to both. The advantage of using an open/short method for initializing the scalar reflectometer has been quantified; it produces a calibration constant very near to unity. On the other hand, the directivity and effective source reflection coefficient of the reflectometer remain as error sources. The worst-case error of a scalar reflectometer measurement depends on the scattering parameters of the reflectometer and the value, |w|, of the measured device. Three different expressions for worst-case error – depending on the scattering parameters of the reflectometer and |w| - were given.

References

[1]D. M. Kerns and R. W. Beatty, Basic Theory of Waveguide Junctions and Introductory Microwave Network Analysis, Pergamon Press, 1967.

[2]G. F. Engen, "Amplitude stabilization of a microwave signal source", IRE Trans. Microwave Theory and Technique, vol. MTT-6, pp. 202-206, April 1958.

[3]U.S. Guide to the Expression of Uncertainty in Measurement, ANSI/NCSL Z540-2-1997, National Conference of Standards Laboratories, Boulder CO

RDM U:\WIN_FILE\WORD.FIL\THEORY PAPERS\Scalar_ref_z3.doc

APPENDIX A

This appendix justifies the expressions for WCE given in equations (17a), (17b) and (17c) - subject to the associated conditions. It also develops the logical conditions for use of the different expressions for WCE. Figure 2 in the body of the report depicted a possible relationship between the loci of w and z. For the purposes of this appendix and convenience, one need consider only the situation when $\arg(C_1) = 0$ as shown in Figure A1.

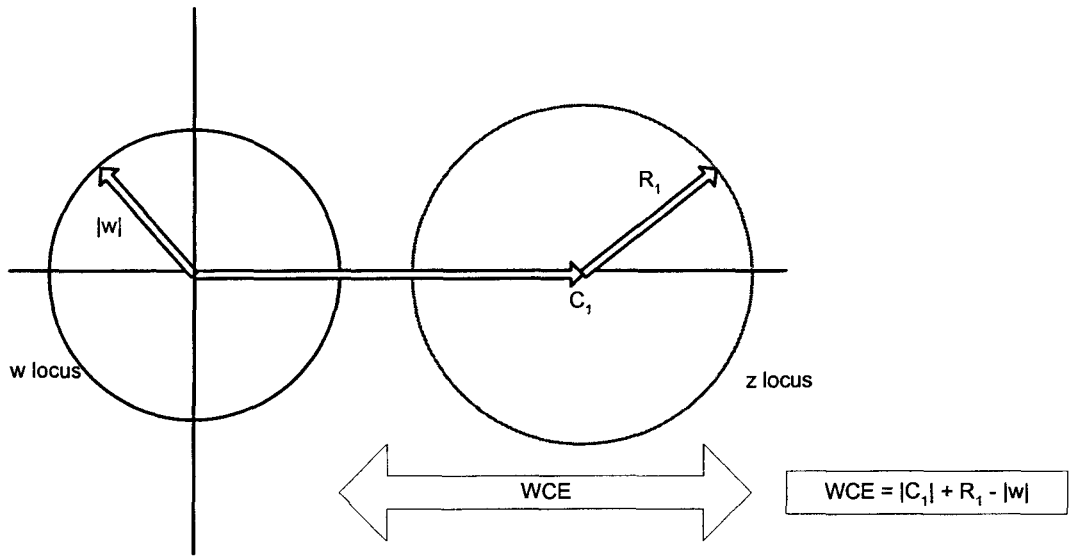

Figure A1. A possible relationship between w and z loci when $\arg(C_1)=0$.

For the sake of even more brevity, all the necessary information in Figure A1 can be condensed into Figure A2.

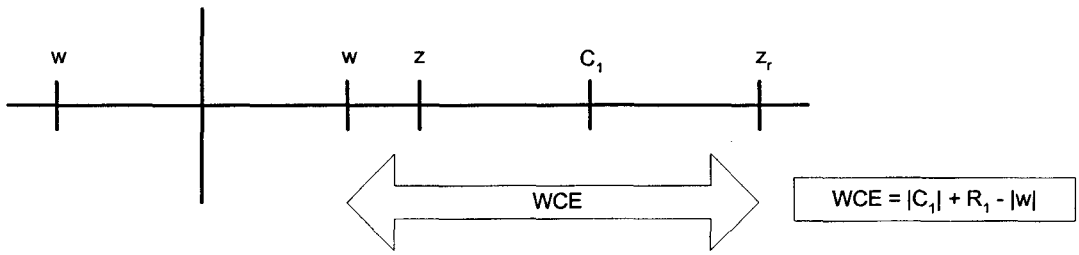

Figure A2. Condition: $|C_1| > R_1 > |w|$

The caption of the figure specifies the size order of $|C_1|$, R_1 and $|w|$. In the figure, the points where the loci intersect the real axis are identified as is the tip of the vector C_1. The center part of Figure A2 graphically shows the worst-case error, WCE, as the distance between (1) the point, z_r, on the z locus that is most remote from the w locus and (2) the point on the w locus that is nearest to z_r. In the right side of the figure, the corresponding algebraic expression for WCE is given. Figures A3 through A7 show corresponding information for the other five order possibilities.

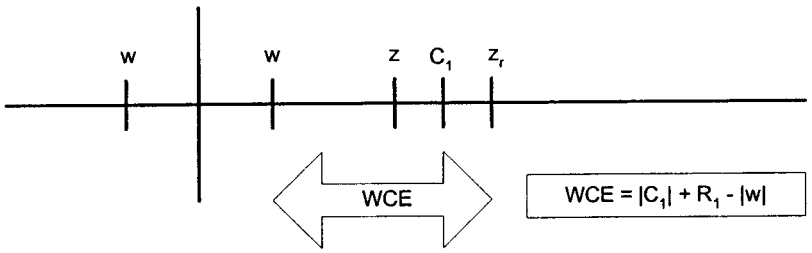

Figure A3. Condition: $|C_1| > |w| > R_1$

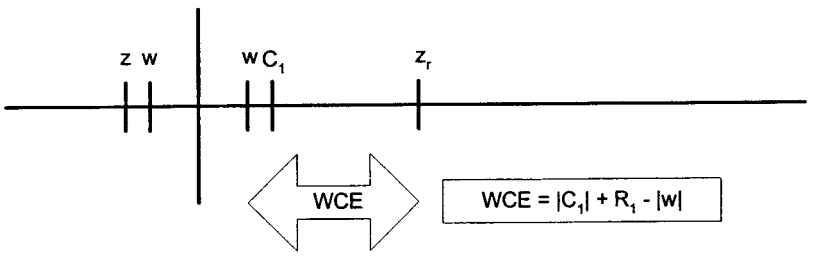

Figure A4. Condition: $R_1 > |C_1| > |w|$

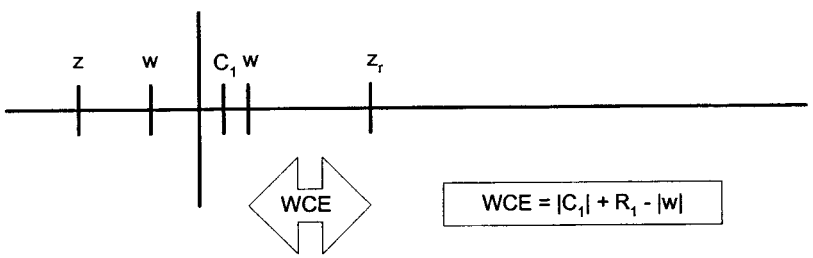

Figure A5. Condition: $R_1 > |w| > |C_1|$

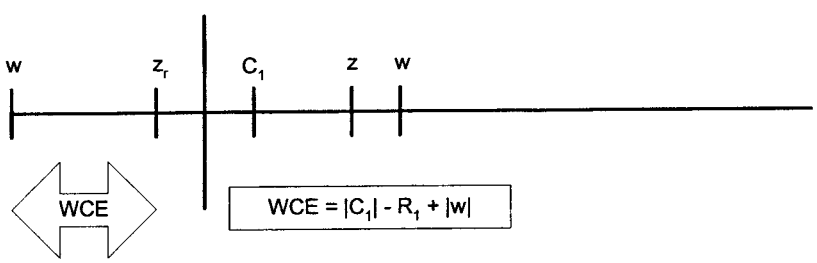

Figure A6. Condition: $|w| > R_1 > |C_1|$

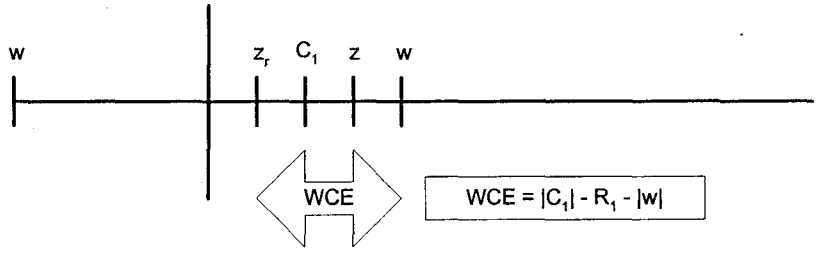

Figure A7. Condition: $|w| > |C_1| > R_1$

In Figures A2 through A5, the same expression is used for the WCE while different expressions are required in Figures A6 and A7. This situation is logically summarized in the Karnaugh map of Figure A8. Notation used is as follows: X identifies a "don't care" or impossible condition. The expression for WCE used in Figures A2 through A5 is identified as expression "1" and is denoted by a leading "1 –". The expression for WCE used in Figure A6 is identified as expression "2" and is denoted by a leading "2 –". The expression for WCE used in Figure A7 is identified as expression "3" and is denoted by a leading "3 –". The figure where each expression appears is indicated as a trailing (for example) "– A7".

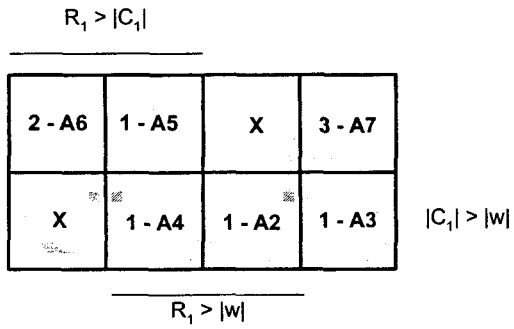

Figure A8. Karnaugh map of expressions for WCE

The map indicates that:
Expression 1 should be used if $R_1 > |w|$ or $|C_1| > |w|$.
Expression 2 should be used if $|w| > R_1$ and $R_1 > |C_1|$ i.e. if $|w| > R_1 > |C_1|$.
Expression 3 should be used if $|w| > |C_1|$ and $|C_1| > R_1$ i.e. if $|w| > |C_1| > R_1$.

DISTRIBUTION:

1 Honeywell FM&T
Attn: Randy Herder
Dept. E14, MS BR28
P. O. Box 419159
Kansas City, MO 64141-6159

1 Los Alamos National Laboratory
Attn: Leo Baca
ESA-AET Standards & Calibration Group
P.O. Box 1663
Los Alamos, NM 87545

1 Pantex Plant
Attn: Mark Kuster
Metrology Bldg 1211B
P.O. Box 30020
Amarillo TX 79177

1 MS 0665 R.B. Pettit, 2542
1 MS 0665 R.J. Haushalter, 2542
1 MS 0665 C.G. Juarez, 2542
15 MS 0665 R.D. Moyer, 2542
1 MS 0665 J.A. Woods, 2542
1 MS 0665 T.F. Wunsch, 2542
1 MS 0665 R.M. Graham, 2542
1 MS 9018 Central Technical Files, 8945-1
2 MS 0899 Technical Library, 9612
1 MS 0612 Review and Approval Desk, 9612
For DOE/OSTI